RHENIUM-OSMIUM GEOCHRONOLOGY

Black carbonaceous shale from outcrop and drill core was sampled from the Callison Lake Formation, Mwashya subgroup (devoid of sulphide mineralization or evidence of fluid flow and from drill core), Taishir and Sheepbed formations. For outcrop samples a ca. 25 cm trench was dug to avoid sampling weathering material similar to methods in Strauss et al. (2014) and to maximize the spread of $^{187}Re/^{188}Os$ values e.g., Kendall et al. (2009). Drill core samples (Zambia) were cut over an interval of 6.49 m and each sample from outcrop and drill core was greater than 30 g yet thinner than 7 cm vertically to minimize variations in initial $^{187}Os/^{188}Os$ values. Although we sampled > 6 m vertically, all initial $^{187}Os/^{188}Os$ values for the Mwashya subgroup displayed very little variation (Table DR1).

Any weathered surfaces were removed with a diamond-encrusted rock saw and samples were then hand-polished using a diamond-encrusted polishing pad to remove cutting marks and eliminate any potential for contamination from the saw blade. The samples were dried overnight at ~60 °C and then crushed to a fine (~30 μm) powder in a SPEX 8500 Shatterbox using a zirconium grinding container and puck in order to homogenize any Re and Os heterogeneity present in the samples (Kendall et al., 2009). Re and Os isotopic abundances and compositions were determined at the Department of Earth and Atmospheric Sciences, University of Houston following methodology by Selby and Creaser (2003) and Cumming et al., (2013).

Between 0.25 and 1 g of sample was digested and equilibrated in 8 ml of $Cr^{VI}O_3$-H_2SO_4 together with a mixed tracer (spike) solution of ^{190}Os and ^{185}Re in carius tubes at

220 °C for 48 hours. Rhenium and osmium was isolated and purified using solvent extraction (NaOH, $(CH_3)_2CO$, and $CHCl_3$,), micro-distillation, anion column chromatography methods, and negative mass spectrometry as outlined by Selby and Creaser (2003) and Cumming et al. (2013). The $Cr^{VI}O_3$-H_2SO_4 digestion method was employed as it has been shown to preferentially liberate hydrogenous Re and Os yielding more accurate and precise age determinations (Selby and Creaser, 2003; Kendall et al., 2004; Rooney et al., 2011). Total procedural blanks during this study were 22.1 ± 4.2 pg and 0.46 ± 0.05 pg for Re and Os respectively, with an average $^{187}Os/^{188}Os$ value of 0.183 ± 0.06 (1σ, n = 4).

Isotopic measurements were performed using a ThermoElectron TRITON PLUS mass spectrometer at the University of Houston via static Faraday collection for Re and ion-counting using a secondary electron multiplier in peak-hopping mode for Os. In-house Re and Os solutions were continuously analyzed during the course of this study to ensure and monitor long-term mass spectrometer reproducibility. The University of Houston Re standard solution measured on faraday cups yields an average $^{185}Re/^{187}Re$ value of 0.59827 ± 0.00158 (1σ, n = 19), which is indistinguishable, within uncertainty to that of Rooney et al. (2010). The measured difference in $^{185}Re/^{187}Re$ values for the Re solution and the accepted $^{185}Re/^{187}Re$ value (0.5974) (Gramlich et al., 1973) is used to correct the Re sample data for instrument mass fractionation and blank and spike contributions. The Os isotope reference material used at NCIET is the Durham Romil Osmium Solution (DROsS) yields an $^{187}Os/^{188}Os$ ratio of 0.10694 ± 0.00051 (1σ, n = 18) that is indistinguishable, within uncertainty, to those reported in (Rooney et al., 2010).

Uncertainties for $^{187}Re/^{188}Os$ and $^{187}Os/^{188}Os$ are determined by error propagation

of uncertainties in Re and Os mass spectrometry measurements, blank abundances and isotopic compositions, spike calibrations, and reproducibility of standard Re and Os isotopic values. The Re-Os isotopic data, 2σ calculated uncertainties for $^{187}Re/^{188}Os$ and $^{187}Os/^{188}Os$, and the associated error correlation function (rho) are regressed to yield a Re-Os date using *Isoplot V. 4.15* with the $\lambda\ ^{187}Re$ constant of $1.666 \times 10^{-11}a^{-1}$ (Ludwig, 1980; Smoliar et al., 1996; Ludwig, 2011).

REFERENCES CITED

Cumming, V.M., Poulton, S.W., Rooney, A.D., and Selby, D., 2013, Anoxia in the terrestrial environment during the late Mesoproterozoic: Geology, v. 41, p.583-586.

Gramlich, J. W., Murphy, T. J., Garner, E. L., and Shields, W. R., 1973, Absolute isotopic abundance ratio and atomic weight of a reference sample of rhenium: Journal of research of the National Bureau of Standards, v. 77A, p. 691-698.

Kendall, B., Creaser, R. A., and Selby, D., 2009, ^{187}Re-^{187}Os geochronology of Precambrian organic-rich sedimentary rocks: Geological Society, London, Special Publications, v. 326, no. 1, p. 85-107.

Ludwig, K. R., 1980, Calculation of uncertainties of U-Pb isotope data: Earth and Planetary Science Letters, v. 46, p. 212-220.

Ludwig, K.R., 2011, Isoplot/Ex, Version 4.15: A geochronological toolkit for Microsoft Excel: Geochronology Center Berkeley, v. 4, p.1-70. http://www.bgc.org/isoplot_etc/isoplot.html.

Rooney, A. D., Selby, D., Houzay, J.-P., and Renne, P. R., 2010, Re-Os geochronology

of a Mesoproterozoic sedimentary succession, Taoudeni basin, Mauritania: Implications for basin-wide correlations and Re-Os organic-rich sediments systematics: Earth and Planetary Science Letters, v. 289, no. 3-4, p. 486-496.

Rooney, A.D., Chew, D.M., Selby, D., 2011, Re-Os geochronology of the Neoproterozoic-Cambrian Dalradian Supergroup of Scotland and Ireland: Implications for Neoproterozoic stratigraphy, glaciation and Re-Os systematics: Precambrian Research, v. 185, p. 202-214.

Selby, D., and Creaser, R. A., 2003, Re-Os geochronology of organic rich sediments: an evaluation of organic matter analysis methods: Chemical Geology, v. 200, no. 3-4, p. 225-240.

Smoliar, M.I., Walker, R.J., Morgan, J.W., 1996, Re-Os ages of Group IIA, IIIA, IVA and IVB iron meteorites: Science, v. 271, p. 1099-1102.

Strauss, J.V., Rooney, A.D., Macdonald, F.A., Brandon, A.D., and Knoll, A.H., 2014, 740 Ma vase-shaped microfossils from Yukon, Canada: Implications for Neoproterozoic chronology and biostratigraphy: Geology, v.42, p.659-662.

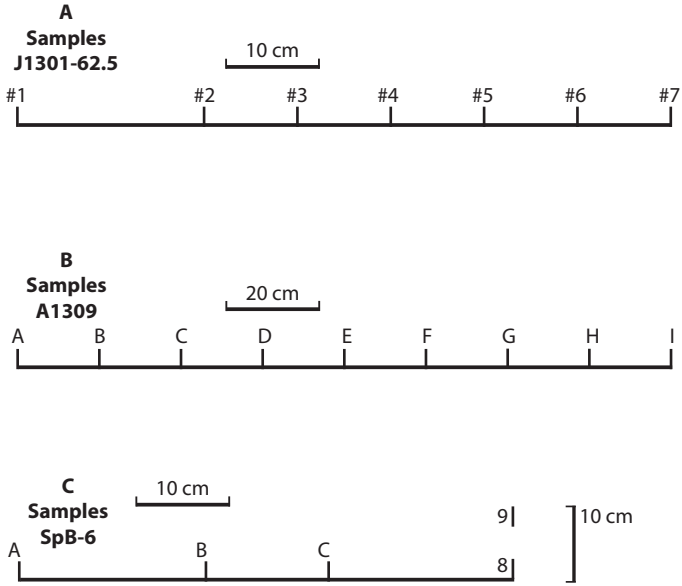

Figure DR1: Schematic diagram of sampling procedures for: A) Callison Lake Formation, sample J1301-62.5 #3 was lost when the carius tube neck broke in the oven and #5 was not processed beyond sample powdering due to time constraints; B) Taishir Formation, samples "G" and "H" were more fissile and broke apart during transport out of the field site and; C) Sheepbed Formation, samples SpB-6 #8 and #9 were part of a vertical transect (height of ca. 1 m) for Os isotope stratigraphy that has not been fully processed yet.

Table DR1: Re and Os elemental abundance data and isotope composition data for all samples Fig. 2A-D

Isochron	Sample	Re (ng/g)	±	Os (pg/g)	±	^{192}Os	±	$^{187}Re/^{188}Os$	±	$^{187}Os/^{188}Os$	±	rho[a]	Os_i[b]
Callison Lake Formation	J1301-62.5-1	11.911	0.110	411.01	1.60	127.34	0.53	186.10	2.17	2.677	0.028	0.702	0.331
GPS co-ordinates:	J1301-62.5-2	17.933	0.120	419.32	1.85	111.35	0.50	320.44	3.18	4.381	0.045	0.789	0.341
N64 39'48.0"	J1301-62.5-4	15.263	0.110	311.05	1.66	76.36	0.48	397.68	3.00	5.355	0.039	0.872	0.341
W139 43'48.6"	J1301-62.5-6	19.278	0.110	430.67	2.24	111.56	0.61	343.83	3.91	4.681	0.040	0.775	0.346
	J1301-62.5-7	22.191	0.130	400.75	2.01	90.41	0.48	488.34	3.00	6.491	0.031	0.877	0.335
Mwashya subgroup	MJ-31	3.296	0.037	54.61	0.43	11.77	0.14	557.18	4.66	7.148	0.069	0.910	0.368
GPS co-ordinates:	MJ-32	8.273	0.080	249.33	1.27	74.63	0.48	220.54	2.46	3.036	0.046	0.957	0.348
Chambishi basin ~	MJ-33	11.599	0.053	240.02	1.21	60.57	0.38	381.02	5.00	5.004	0.063	0.925	0.361
N12 15'00.0"	MJ-34	14.027	0.067	255.91	1.33	59.60	0.37	468.24	6.17	6.052	0.076	0.925	0.346
E28 20'00.0"	MJ-35	11.926	0.171	387.54	1.91	118.56	0.65	200.15	2.14	2.808	0.043	0.749	0.369
	MJ-36	7.947	0.126	174.65	1.07	45.57	0.33	347.00	5.38	4.593	0.081	0.739	0.365
	MJ-37	0.826	0.072	37.76	0.47	12.62	0.32	130.27	6.13	1.931	0.036	0.800	0.343
Taishir Formation	A1309-A	0.928	0.005	55.26	0.20	18.97	0.08	97.34	1.09	1.680	0.013	0.863	0.600
GPS co-ordinates:	A1309-B	1.885	0.008	95.70	0.36	32.12	0.13	116.77	1.22	1.891	0.014	0.969	0.596
N46 40'20.1"	A1309-C	1.042	0.004	60.30	0.22	20.63	0.09	100.45	1.12	1.712	0.015	0.964	0.598
E96 33'39.5"	A1309-D	9.644	0.048	328.34	1.36	101.62	0.41	188.82	1.99	2.688	0.025	0.885	0.594
	A1309-E	3.720	0.015	164.98	0.65	54.06	0.22	136.92	1.44	2.121	0.022	0.942	0.602
	A1309-I	5.718	0.024	153.99	0.69	44.44	0.18	256.00	2.69	3.428	0.037	0.968	0.589
Sheepbed Formation GPS	SpB-6A	14.85	0.074	316.77	1.92	78.94	0.34	374.38	3.80	5.163	0.050	0.845	1.213
co-ordinates: N64	SpB-6B	5.45	0.028	371.99	0.99	121.46	0.23	89.29	0.91	2.155	0.050	0.923	1.213
29'50.4"	SpB-6C	6.15	0.089	106.96	0.53	23.89	0.11	512.09	5.64	6.635	0.060	0.966	1.232
W129 25'42.0"	SpB-6-8	12.21	0.076	204.59	0.90	44.72	0.14	543.29	6.00	6.943	0.070	0.829	1.210
	SpB-6-9	12.08	0.150	276.39	2.24	70.86	0.66	339.17	5.68	4.808	0.017	0.784	1.218

Uncertainties are given as 2σ for $^{187}Re/^{188}Os$ and $^{187}Os/^{188}Os$ and ^{192}Os.

The uncertainty includes the 2 SE uncertainty for mass spectrometer analysis plus uncertainties for Os blank abundance and isotopic composition.

Ages are calculated using the $\lambda^{187}Re = 1.666 \times 10^{-11} y^{-1}$ (Smoliar et al., 1996).

[a] Rho is the associated error correlation (Ludwig, 1980).

[b] Os_i = initial $^{187}Os/^{188}Os$ isotope ratio calculated at 753 Ma, 727 Ma, 659 Ma and 632 Ma for the Callison Lake Formation, Mwashya subgroup and Taishir and Sheepbed formations, respectively.

All GPS coordinates are in datum WGS 84

Table DR2: Geological age constraints, techniques and data sources

Paleocontinent	Age (Ma)	(+)	(-)	Technique	Grains	Relationship to Glacial Deposit	Number	Reference
South China	632.5	0.5	0.5	U-Pb ID-TIMS	magmatic	above Nantuo	1	Condon et al., 2005, Science, v.**308**, p. 95-98
South China	632.5	1.0	1.0	U-Pb ID-TIMS	magmatic	above Nantuo	2	Schmitz, M.D., Geological Time Scale 2012, v. **2**, p. 1045-1082 - recalculation of above date
Laurentia	632.3	5.9	5.9	Re-Os	isochron	above Ice Brook	3	This paper
Kalahari	635.5	0.5	0.5	U-Pb ID-TIMS	magmatic	within Ghuab	4	Hoffmann et al., 2004, Geology, v.**32**, p. 817-820
Kalahari	635.5	1.1	1.1	U-Pb ID-TIMS	magmatic	within Ghuab	2	Schmitz, M.D., Geological Time Scale 2012, v. **2**, p. 1045-1082 - recalculation of above date
South China	636.3	4.9	4.9	U-Pb SHRIMP	magmatic	within Nantuo	5	Zhang et al., 2005, Geology, v. **33**, p. 473-476
Australia	636.4	0.5	0.5	U-Pb ID-TIMS	magmatic	above Cottons Breccia	6	Calver et al., 2013, Geology, v. **41**, p. 1127-1130
Australia	640.7	5.7	5.7	Re-Os	isochron	possibly above Sturtian	7	Kendall et al., 2009, Precambrian Research, v. **172**, p. 301-310
South China	654.5	3.8	3.8	U-Pb SHRIMP	magmatic	below Nantuo	5	Zhang et al., 2005, Geology, v. **33**, p. 473-476
Australia	657.2	6.9	6.9	Re-Os	isochron	above Sturtian below Marinoan	8	Kendall et al., 2006, Geology, v. **34**, p. 729-732
Mongolia	659.0	4.5	4.5	Re-Os	isochron	1m above Maikhan Ul	3	This paper
Laurentia	659.6	10.2	10.2	Re-Os	isochron	below Port Askaig	9	Rooney et al., 2011,Precambrian Research, v. **185**, p. 202-214
Laurentia	662.4	4.6	4.6	Re-Os	isochron	above Rapitan	10	Rooney et al., 2014, Proceedings of the National Academy of Sciences, v. **110**, p. 51-56.
South China	662.9	4.3	4.3	U-Pb ID-TIMS	magmatic	below Nantuo above Tiesiao	11	Zhou et al., 2004, Geology, v. **32**, p. 437-440.
Laurentia	684.0	4.0	4.0	U-Pb SHRIMP	magmatic	unknown	12	Lund et al., 2003, Geological Society of America Bulletin, v. **115**, p. 349-372
Laurentia	685.0	7.0	7.0	U-Pb SHRIMP	magmatic	unknown	12	Lund et al., 2003, Geological Society of America Bulletin, v. **115**, p. 349-372
Laurentia	685.5	0.4	0.4	U-Pb ID-TIMS	magmatic	within lower Scout Mountain	13	Keeley et al., 2013, Lithosphere, v. **5**, p. 128-150
Laurentia	687.4	1.3	1.3	U-Pb ID-TIMS	magmatic	unknown	14	Condon and Bowring, 2011, Geological Society, London, Memoirs, Chapter v. **36**, p. 135-149
Laurentia	688.6	9.5	6.2	U-Pb ID-TIMS	magmatic	within Rapitan	15	Ferri et al., 1999, British Columbia Ministry of Energy and Mines, Bulletin, v. **107**, p.1-122
Laurentia	709.0	5.0	5.0	U-Pb SHRIMP	magmatic	unknown	16	Fanning and Link, 2004, Geology, v. **32**, p. 881-884
Arabia	711.5	0.3	0.3	U-Pb ID-TIMS	magmatic	within Ghubrah	17	Bowring et al., 2007, American Journal of Science, v. **307**, p. 1097-1145
South China	715.8	2.5	2.5	U-Pb ID-TIMS	magmatic	below Chang'an	18	Lan et al., 2014, Precambrian Research, v. **255**, p. 401-411
Laurentia	716.5	0.2	0.2	U-Pb ID-TIMS	magmatic	within Rapitan	19	Macdonald et al., 2010, Science, v. **327**, p. 1241-1243
Laurentia	717.4	0.1	0.1	U-Pb ID-TIMS	magmatic	below Rapitan	19	Macdonald et al., 2010, Science, v. **327**, p. 1241-1243
Laurentia	719.5	0.3	0.3	U-Pb ID-TIMS	magmatic	base of Hula Hula	20	Cox et al., in review, Lithosphere
Arabia	726.0	1.0	1.0	U-Pb ID-TIMS	magmatic	Leger granite	17	Bowring et al., 2007, American Journal of Science, v. **307**, p. 1097-1145
Congo	727.3	4.9	4.9	Re-Os	isochron	below Grand Conglomerate	3	This paper
Laurentia	732.2	4.7	4.7	Re-Os	isochron	below Rapitan	10	Rooney et al., 2014, Proceedings of the National Academy of Sciences, v. **110**, p. 51-56.
Congo	735.0	5.0	5.0	U-Pb SHRIMP	magmatic	below Kundelungu	21	Key et al., 2001, Journal of African Earth Sciences, v. **33**, p. 503-528
Laurentia	736.0	23.0	17.0	U-Pb ID-TIMS	magmatic	below Rapitan	22	McDonough and Parrish, 1991, Canadian Journal of Earth Sciences, v. **28**, p. 1202-1216
Laurentia	739.9	6.5	6.5	Re-Os	isochron	below Rapitan	23	Strauss et al., 2014, Geology, v. **42**, p. 659-662
Kalahari	741.0	6.0	6.0	Pb-Pb ID-TIMS	magmatic	below Numees	24	Frimmel et al. 1996, The Journal of Geology, v. **104,** p. 459-469
Laurentia	742.0	6.0	6.0	U-Pb ID-TIMS	magmatic	top of Chuar	25	Karlstrom et al., 2000, Geology, v. **28**, p. 619-622
Laurentia	752.7	5.5	5.5	Re-Os	isochron	below Rapitan	3	This paper

All age uncertainties are 2σ.
ID-TIMS, Isotope-Dilution Thermal Ionization Mass Spectrometry
SHRIMP, Sensitive High Resolution Ion Microprobe
SIMS, Secondary Ion Mass Spectrometry